Transversal and Lateral Exciton Energy Transfer in Grana Thylakoids of Spinach†

Helmut Kirchhoff,*,‡ Mauricio Borinski,‡ Steven Lenhert,§ Lifeng Chi,§ and Claudia Büchel‖

Institut für Botanik, Schlossgarten 3, and Physikalisches Institut, Wilhelm-Klemm-Strasse 10, D-48149 Münster, Germany, and Max-Planck-Institut für Biophysik, Marie-Curie-Strasse 15, D-60439 Frankfurt am Main, Germany

Received July 17, 2004; Revised Manuscript Received August 27, 2004

ABSTRACT: The excitation energy transfer between photosystem (PS) II complexes was studied in isolated grana disks and thylakoids using chlorophyll *a* fluorescence induction measurements in the presence of DCMU under stacked and destacked conditions. Destacking of grana was achieved using a sonication protocol in a buffer without $MgCl_2$. The degree of stacking was controlled and quantified by atomic force microscopy and by the concomitant absorption changes. As expected from the literature, intact thylakoids showed a strong dependency of the connectivity of PSII centers, the F_m/F_o ratio as well as the fraction of PSIIβ centers on the $MgCl_2$ concentration. In contrast, these parameters did not change in isolated grana disks. In particular, the connectivity remained constantly high irrespective of the degree of destacking. These differences were explained by the high protein density in grana disks, which hinders separation and mixing of proteins sufficiently to change energy transfer properties. Due to the occurrence of stroma lamella in intact thylakoids, intermixing of PSII and PSI is possible and allows for changes in F_m/F_o ratio as is the separation of LHCII from PSII, thus leading to an increase in the fraction of PSIIβ. Even if mixing and separation of proteins are impaired in isolated grana disks, destacking should lead to a decrease in connectivity if transversal excitation energy transfer between two opposite membranes is significant. Because the connectivity is constant over all degrees of destacking employed, we conclude that the energy transfer in granas is mainly lateral.

Light harvesting is of vital significance for all photosynthetic organisms. This function is realized by highly specialized proteins, light harvesting protein complexes (LHCs), and core antenna proteins. These proteins bind the light absorbing pigments, such as chlorophylls (*1*, *2*). Absorbed light energy is transferred inside and among LHCs by nonradiative exciton transfer to the photochemically active traps of the photosystems (reaction centers, RC)[1] (*3*). Here the energy of the excited state is converted into redox energy (primary charge separation) that is finally used for the formation of ATP and NADPH + H^+. An extended light harvesting antenna system is built up from the functional cooperation of many LHCs. This results in an enlargement of the apparent absorption cross section per RC by a factor of 100−1000, which forms the basis of efficient light harvesting. In various photosynthetic organisms (green bacteria, purple bacteria, cyanobacteria, red algae, or higher plants) the antenna systems are remarkably diverse. However, in higher plants all LHCs are members of the *cab*-gene family, which share a high sequence homology (*4*). They are characterized by three transmembrane helices and are integral components of the thylakoid membrane system in chloroplasts.

The thylakoid membrane is subdivided in two compartments: About 80% of the membrane (*5*) is organized in strictly stacked grana membranes which are connected by unstacked stroma lamellae (*6*). The main integral proteins of the thylakoid are, in addition to the LHCs, the two photochemically active photosystems I and II, the cytochrome *bf* complex, and the ATPase (*6*). Today, a detailed picture of the organization of the protein complexes in the thylakoid membrane exists due to a huge number of structural investigations. The protein complexes, which can consist of up to 30 different subunits, can assemble into relatively stable higher associations named supercomplexes (*7*−*10*). From functional considerations of the energy transfer in PSII and PSI the term photosynthetic unit (PSU) was introduced, which can be defined as a structural entity consisting of the reaction center and its associated antenna system (*11*, *12*). It is likely that supercomplexes are the structural representation of the PSUs. The organization of the PSUs of PSII and PSI is quite different. Beside the fact that PSI has a RC of the iron−sulfur type and PSII has a quinone type RC (*13*), the antenna systems show significant differences (*13*). Most of the antenna chlorophylls of PSI are bound to core complexes (*8*). The complete PSU of PSI consists of four LHCI subunits (*8*) and possibly additional LHCIIs (*14*). PSI is exclusively localized in unstacked thylakoid regions (*14*). For PSII the situation is more complex. The mainstream concept for the antenna organization of PSII postulates two types of photosystems, PSIIα and PSIIβ (*15*). It is assumed that the PSU for PSIIβ consists of the core antenna CP43 and CP47 as well as the minor LHCs CP24, CP26, and CP29

† H.K. and C.B. are supported by the Deutsche Forschungsgemeinschaft (KI 818/2-1, Bu 812/2-2).

* Corresponding author. Phone: +49 251 8324820. Fax: +49 251 8323823. E-mail: kirchhh@uni-muenster.de.

‡ Institut für Botanik.

§ Physikalisches Institut.

‖ Max-Planck-Institut für Biophysik.

[1] Abbreviations: chl, chlorophyll; DCMU, 3-(3,4-dichlorophenyl)-1,1-dimethylurea; F_o, chlorophyll *a* fluorescence level with oxidized QA; F_m, fluorescence level with completely reduced QA; F_v, variable part of the fluorescence; PS, photosystem; PSU, photosynthetic unit; QA, primary quinone acceptor of photosystem II; RC, reaction center.

10.1021/bi048473w CCC: $27.50
Published on Web 10/23/2004

(*Lhcb* 4, 5, and 6) (*1*), which altogether bind about 100 chlorophylls. There is good evidence for a monomeric organization of PSIIβ in thylakoids (*15*). The majority of PSII is of the PSIIα type that binds various numbers of additional LHCII trimers (*Lhcb* 1−3 gene products). This results in a two to three times bigger antenna (200−250 chlorophylls per RC) compared to PSIIβ. There are good indications that PSIIα is exclusively localized in stacked grana regions and is organized as a dimeric supercomplex (*16*). The progress in the structural elucidation of protein complexes in thylakoids forms the basis for a deeper biophysical understanding of energy migration and photochemical trapping in PSII and PSI (*17*−*19*).

An important difference between PSIIα and PSIIβ and PSI is the fact that in the case of PSIIα several PSUs are excitonically connected (e.g., ref *12*). This phenomenon is named connectivity and enables a better utilization of light energy by PSIIα: Light quanta absorbed by a PSU that is photochemically inactive (e.g., the primary quinone acceptor, QA, is in the reduced state) can be used by a neighboring PSU with an oxidized QA via interunit exciton transfer. This connectivity is associated with grana stacking. Grana can be destacked in vitro by incubating thylakoids in media with low ionic strength, e.g., without Mg^{2+} cations (*20, 21*). Destacked thylakoids show a significant decrease in the connectivity between PSIIα (*22*). The structural realization of the connectivity phenomenon on the supramolecular level in grana stacks is under debate. It is likely that the excitonic coupling between PSUs is mediated by LHCII. In principle, this coupling can occur by lateral exciton transfer within a grana disk or by transversal transfer between opposite grana disks. Both possibilities were suggested in the literature (*23, 24*). The experimental evidence for a transversal energy transfer is rather low. From fast photovoltage measurements it was concluded that it could exist in stacked thylakoids (*25*). However, the evidence is rather indirect, and the author discusses also alternative explanations (*25*). So far there is no direct evidence that both lateral and transversal exciton transfers are realized in grana stacks. Electron microscopy on isolated grana membranes gave evidence for some parts of grana membranes that only contain LHCII. Next to these areas crystalline arrays of PSIIα are found, as well as in the opposite membrane sheet. As the size of the LHCII-only areas is too large to allow for efficient lateral energy transfer, it was concluded that transversal energy transfer has to take place (*26*). The question whether a transversal energy transfer is possible is even more relevant for a recently postulated alternative structural model of the protein organization in grana stacks (*27*). In this model two types of homogeneously built membranes strictly alternate in the grana disks. One type contains only PSII cores whereas the other type contains solely LHCII complexes. In this organization efficient light harvesting requires transversal energy transfer from the LHCII-only membranes to the opposing membrane, which contains the PSII centers. In this work we analyze the significance of transversal exciton transfer between opposite disks in isolated grana membranes prepared according to ref *28* (BBY membranes). BBY membranes consist of flat paired membranes originating from the core region of the grana together with different amounts of grana margins (*29*). Recently, it was shown that in BBY membranes the protein density and organization are similar to grana of intact chloroplasts (*30*). Thus, this type of preparation is useful to analyze both lateral and transversal energy transfer in the antenna system of PSII.

Here we examine the contribution of transversal exciton transfer by a functional comparison of stacked versus unstacked grana, exploiting the fact that no transversal energy transfer is possible after destacking. For unstacking a protocol was developed on the basis of sonication of membranes in media of low ionic strength. The degree of stacking under both stacked and destacked conditions was quantified by atomic force microscopy (AFM). The functional analysis of energy transfer in the PSII antenna was examined by chlorophyll *a* fluorescence induction measurements.

Chlorophyll *a* fluorescence induction is a sensitive, noninvasive, and well-established method for analyzing the energy utilization in PSII (*11*, *31*). Lavergne and Trissl developed a sophisticated mathematical description for analyzing induction kinetics (*32*) which is based on the commonly accepted exciton radical pair equilibrium model for PSII (*3*). Besides other parameters this analysis provides the quantity J, which is a measure of the connectivity between PSUs of the PSIIα type. The value $(1 + J)$ can be interpreted as the relative enlargement of the antenna of an open PSIIα (oxidized QA) by interunit exciton transfer if all neighboring PSUs are closed (reduced QA) (*32*). Thus, a decrease in J upon destacking of grana membranes is indicative of a significant contribution of transversal exciton energy transfer in stacked grana thylakoids.

MATERIALS AND METHODS

Membrane Preparations and Destacking of Grana Thylakoids. Thylakoids were isolated from 6 week old leaves of spinach (*Spinacea oleracea* var. polka) grown hydroponically (*33*) at 13−16 °C according to ref *34*. The photoperiod was 10 h (300 μmol of quanta m^{-2} s^{-1}). Grana thylakoids were isolated from the chloroplasts according to ref *28* (BBY membranes) with slight modifications described in ref *30*. The chlorophyll content was determined according to ref *35*.

Several conditions were tested to destack isolated grana membranes. Atomic force microscopy and absorption changes at 505 nm (see Results) were used to check the degree of stacking. No quantitative destacking could be reached by either incubating the BBY membranes over several hours in $MgCl_2$-free buffer with EDTA or an additional treatment in a sonicator bath (low energies). However, a nearly complete unstacking was achieved by treating BBYs for 1 min with an ultrasonic tip (30 W) in buffer containing 0.5 mM EDTA, 10 mM KCl, and 15 mM 2-(*N*-morpholino)ethanesulfonic acid (MES) (pH 6.5, KOH) at 4−8 °C and a chlorophyll concentration of 10 μmol·L^{-1}. For control membranes and for partly destacked membranes due to different $MgCl_2$ concentrations, EDTA was replaced by 7 mM $MgCl_2$ or the indicated $MgCl_2$ concentrations, respectively. The membranes were stored on ice for at least 20 min prior to use.

Destacking of intact thylakoids was achieved as described in ref *36*. In detail thylakoids were adjusted to 2 mg of chlorophyll·mL^{-1}. The membranes were diluted 1:1 in 0.5 mM EDTA, 5 mM KCl, and 10 mM *N*-(2-hydroxyethyl)-piperazine-*N*′-2-ethanesulfonic acid (HEPES, pH 7.6) and incubated for 1 h on ice under slow stirring. The membranes were then again diluted 1:100 in the same buffer and stored

on ice until use (10 μmol·L^{-1} final chlorophyll concentration). For the $MgCl_2$ series EDTA was replaced by the indicated $MgCl_2$ concentrations. Control thylakoids were directly diluted in a buffer with 330 mM sorbitol, 80 mM KCl, 7 mM $MgCl_2$, and 25 mM HEPES (pH 7.6, KOH).

Atomic Force Microscopy (AFM). AFM (Digital Instruments, Dimension 3000, Santa Barbara, CA) was performed in air using the tapping mode with silicon cantilevers (nanosensors) with resonant frequencies of 250−350 kHz and nominal spring constants of ~42 N/m. Samples were prepared by placing a 50 μL drop of stacked or destacked grana membranes on a freshly cleaved mica surface (~7 × 7 mm) for 2 min prior to rinsing 10 times (100 μL/rinse) with Millipore water (resistivity 18.2 MΩ·cm) in order to remove the buffer. The sample was then dried under a nitrogen stream for 2 min. Qualitative comparisons between samples prepared with and without the rinsing step indicated that rinsing the adsorbed membranes with pure water had no obvious effect on the stacking of the membranes.

Chlorophyll a Fluorescence Induction. Induction curves were measured in a laboratory-built fluorometer. Broad green excitation light was produced by a halogen lamp filtered through Corning 9782, BG 18, and heat mirror filters. The light was guided on the entrance of a mirrored cuvette (dimensions 5 × 5 mm) protected with a fast electronic shutter (0.7 ms opening time, LS6T2, Uniblitz Co., Dietzenbach, Germany). The fluorescence light at 90° was filtered by Schott RG695 and Calflex C filters and detected with a photomultiplier with a red-sensitive photocathode (R636-10, Hamamatsu). The photomultiplier signal was recorded with an analog to digital converter computer card and processed with a self-written software program (vKD Mess- and Prüfsysteme, Kürten-Engeldorf, Germany).

BBY membranes or thylakoids were incubated in buffers described above at a chlorophyll concentration of 10 μmol·L^{-1}. The F_o level was measured after 15 min of incubation in strict darkness. With the same probe the F_m level was detected after addition of 1 mM sodium dithionite. Dithionite was added to avoid fluorescene quenching by oxidized plastoquinone. In a separate experiment the fluorescence induction kinetics in the presence of DCMU were measured. After incubating the membranes in strict darkness for at least 15 min, 1 mM NH_2OH (to compensate for possibly damaged donor sides) and 20 μM DCMU were added and the induction kinetics recorded after 1−2 min.

Fluorescence induction kinetics were analyzed on the basis of the connected units model as described in ref *32*. The analysis of the normalized variable fluorescence, F_v, provides the rate constants k_α and k_β for QA reduction (proportional to the apparent antenna size of a PSU) of PSIIα and PSIIβ, respectively. In addition, the relative proportion of PSIIβ fluorescence and the connectivity parameter J for PSIIα can be deduced. For these calculations an iterative fitting procedure was employed. First, theoretical fluorescence induction curves for PSIIα ($F_v\alpha$) were calculated using a given k_α and J parameter set and eq 11 taken from ref *32*. The measured F_v signal was then fitted with the equation (program SigmaPlot):

$$F_v(t) = A_\beta(1 - e^{-tk\beta}) + (1 - A_\beta)F_v\alpha(t) \qquad (1)$$

where $F_v(t)$ is the variable fluorescence level at time t, A_β is the relative fraction of PSIIβ fluorescence, and k_β and k_α are the rate constants for QA reduction in PSIIβ and PSIIα, respectively.

In these calculations, A_β and k_β were freely adjustable parameters. After fitting, the residuals were calculated, and another routine was conducted with a new k_α and J parameter set. From the plot of the residuals versus k_α and J the best parameter set was extracted (where the residuals are minimal). An example for a fit is given in Figure 4.

Absorption Measurements. Salt-induced changes of absorption spectra indicate aggregation of LHCII (e.g., ref *37*) and are used to monitor the degree of stacking of grana (see Results). Absorption spectra from 400 to 800 nm were recorded in a Hitachi 3010 photometer with a slit width set to 1 nm and a scanning speed of 300 nm/min. Salt-induced absorption changes were demonstrated by the difference of the spectrum of grana membranes sonicated in the presence of the indicated $MgCl_2$ concentration minus the spectrum of untreated membranes in the presence of 7 mM $MgCl_2$. To account for slightly different chlorophyll concentrations, the spectra were normalized to the absorption maximum around 675 nm before subtraction. Therefore, the data in Figure 2 represent absorption changes relative to the maximum absorption around 675 nm.

The P700 content was determined using the light-induced absorption changes at 810 nm minus the changes at 860 nm (unpublished experiments and ref *38*). Thylakoids or BBY membranes were suspended in a buffer containing 5 mM $MgCl_2$, 30 mM KCl, 300 mM sorbitol, 50 mM citrate (pH 4.8), and 0.2% (w/v) dodecyl β-maltoside at a chlorophyll concentration of 40 μmol·L^{-1}. Before the measurements 100 μM methyl viologen and 1 mM sodium ascorbate were added. The P700 content was calculated from the maximal absorption change induced by a 150 ms red light pulse (Schott RG 645).

Calculation of Förster Transfer Rates. Distances between neighboring chlorophylls inside LHCII (PDB file 1RWT) were measured using the program O (*39*) for all chlorophylls present. Calculations of Förster transfer rates were done using the formulas provided by ref *19*.

RESULTS

Degree of Stacking of Grana Membranes Investigated by Atomic Force Microscopy (AFM). Figure 1 shows examples of AFM images measured on sonicated grana membranes under stacked or destacked conditions. From topographic sections (gray lines at the top of Figure 1 and the corresponding height profiles at the bottom) it is obvious that the structures are rather flat and are characterized by a sharp rise from the mica surface (black) to the level of the structures (gray). Both parameters are good indications for biomembranes as, e.g., the topographic profile of small water drops shows a sine-like characteristic (not shown). Furthermore, within a few hundred nanometers the diameter of a membrane disk corresponds to the dimension of grana thylakoids (*40*). Additionally, topographic substructures such as patchy surfaces and indentations in the height profiles can be recognized. It can be estimated that these structures with a diameter of about 20 nm extrude about 2−4 nm from the membrane surface of 4−5 nm, resulting in a maximal height of about 8 nm (Figure 1B). Thus it is possible that these

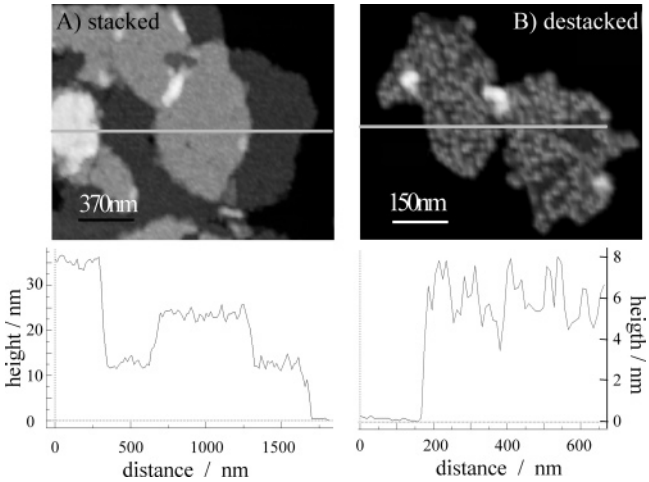

FIGURE 1: Atomic force micrographs of grana membranes. The membranes were either incubated under stacked (A) or destacked (B) conditions. The gray lines indicate the position of the height profile shown at the bottom. The level of the mica surface (black) was set to zero. Note the patchy structures in panel B. For further details see the text.

substructures represent PSII supercomplexes where the water splitting complex is oriented toward the AFM tip (*10*). It is noteworthy that interactions between the AFM tip and the sample can distort the apparent topography (see Discussion). Thus, the dimensions must be taken as a rough estimate. However, in this work we are interested in the mean height of grana membranes under stacked and destacked conditions. Statistical analyses of the height distributions are given in Figure 2. The histograms were fitted with Gaussians (Figure 2). The relative proportion of membranes with a particular mean height was then deduced from integrating the curves. For 61% of stacked grana a mean height of 11.9 nm, for 32% 22.4 nm, and for 7% 33.5 nm was calculated; 73% of destacked grana have a height of 6.8 nm, 20% of 11.8 nm, and 7% of 17.8 nm.

A single lipid bilayer has a thickness of 4.6−6.7 nm (*41*) depending on the type of lipid. The height of the LHCII trimer is 4.8 nm (*48*). It was suggested that the thickness of the thylakoid lipid bilayer is about 5.5 nm (*40*). Thus the mean value of 6.8 nm determined for grana measured under destacked conditions is slightly higher than expected for a single, unpaired grana membrane. This difference can easily be explained by the increase of the mean height due to extrinsic parts of the membrane proteins, especially the subunits of PSII shielding the water splitting system (see above). Considering that a single grana membrane has a mean height of 6−7 nm, the discrete height distribution in Figure 2 can easily be understood: For destacked conditions the height of 11.8 and 17.8 nm represents two and three single layers, loosely associated by lying on top of each other on the mica surface. In contrast, under stacked conditions obviously only multiples of paired grana membranes of 11.9 nm occur (22.4 and 33.5 nm). This is in accordance with electron microscopic studies on BBY membrane preparations in the presence of $MgCl_2$ (*29*). In summary, we conclude that grana membranes incubated in order to preserve stacking are organized as pairs of two membranes, whereas under the conditions for unstacking used here mainly single layer membranes are present.

$MgCl_2$-Dependent Stacking of Grana Measured by Absorption Changes. It is assumed that LHCII is the protein mainly responsible for grana stacking (*23*). Salt-induced aggregation of the LHCII is accompanied by characteristic absorbance changes (e.g., ref *37*). These changes might reflect light scattering changes and flattening effects (*42*). However, we used these signals as a relatively simple tool to investigate $MgCl_2$-induced changes in grana stacking, calculating difference spectra of nonsonicated grana in the presence of 7 mM $MgCl_2$ minus grana sonicated at a given $MgCl_2$ concentration. A typical difference spectrum for a sample sonicated without $MgCl_2$ is shown in the inset of Figure 3. This spectrum is in good accordance with difference spectra that are associated with LHCII stacking (*37*, *43*). For monitoring $MgCl_2$-dependent changes in grana stacking, the height of the characteristic absorption change at 505 nm is plotted against the salt concentration (Figure 3).

It is noteworthy that sonication of membranes alone, without further change in $MgCl_2$ concentration (7 mM $MgCl_2$), already leads to the appearance of a signal at 505 nm (Figure 3). It is likely that this is caused by unspecifically associated grana stacks being present, which are separated by the sonication without dissociation of the grana pairs (see AFM analysis). However, a decrease in the $MgCl_2$ concentration causes a further increase in the absorption signal (Figure 3). On the basis of the analogy to the results with isolated LHCII (*37*) and of the AFM analysis, we conclude that the $MgCl_2$-dependent changes reflect destacking of paired grana. From Figure 3 it follows that 50% of stacked grana are destacked at about 0.2 mM $MgCl_2$.

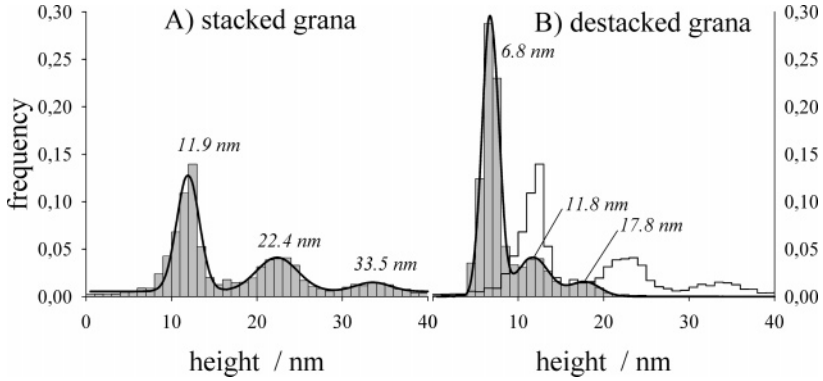

FIGURE 2: Statistical analysis of the grana height. The data were collected from 16 stacked and 19 destacked grana patches as shown in Figure 1. For the histograms the pixels of an entire grana patch were analyzed. Histograms were fitted with three Gaussians (bold lines) to deduce the mean height and the relative contribution. The white histogram in panel B indicates the profile of stacked grana (panel A).

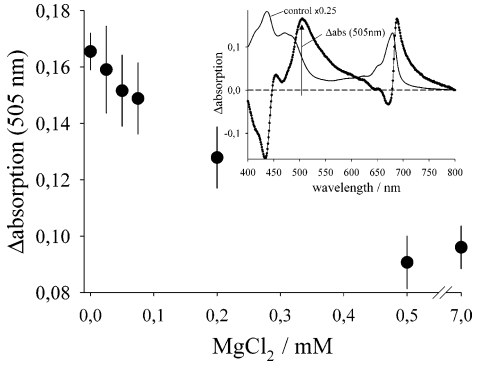

FIGURE 3: Dependence of absorption changes on the $MgCl_2$ concentration. The data represent the difference between untreated grana membranes at 7 mM $MgCl_2$ and grana membranes sonicated in the presence of the indicated $MgCl_2$ concentration. The spectrum of untreated membranes (control) and the difference spectrum (without $MgCl_2$) are shown in the inset. The characteristic signal change at 505 nm was used to quantify the absorption change. Vertical bars indicate the standard deviations. The data are the mean of six independent determinations.

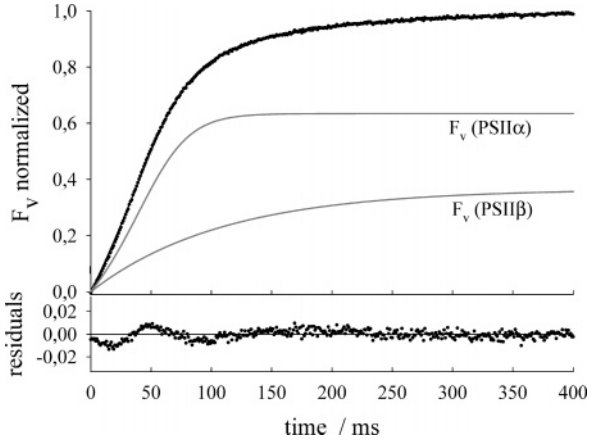

FIGURE 4: Example for a chlorophyll *a* fluorescence induction and its analysis. The curve shows the light-induced increase of the normalized variable fluorescence (F_v) which reflects QA reduction measured with grana membrane (7 mM $MgCl_2$) in the presence of 20 μM DCMU and 1 mM NH_2OH. The curve was fitted with eq 1. The resulting F_v curves for PSIIα, F_v(PSIIα) and PSIIβ, F_v(PSIIβ) are shown. Deviation of the fitted curve from the measured data is depicted at the bottom (residuals). Values of the fitted parameters: $k_\alpha = 0.0210\ s^{-1}$; $k_\beta = 0.0092\ s^{-1}$; $A_\beta = 0.37$; $J = 1.50$.

Chlorophyll a Fluorescence Induction of Stacked and Destacked Membranes. A chlorophyll *a* fluorescence induction curve measured on BBY membranes and its analysis are shown in Figure 4. As explained in Materials and Methods this analysis is based on the PSIIα/PSIIβ heterogeneity (*15*, *31*). Additionally, it is assumed that the energy migration and photochemical trapping in PSIIα function according to the connected units model and for PSIIβ functions according to the separate units model (*12*, *32*). The parameters for PSIIα and PSIIβ deduced from this analysis are summarized in Figure 5 for BBY membranes (left) and intact thylakoids (right) as a function of the $MgCl_2$ concentration.

The comparison of the stacked control probes for BBYs and thylakoids (at 7 mM $MgCl_2$) reveals that all parameters have similar values. It is surprising that the BBY preparation has a similar proportion of PSIIβ compared to intact thylakoid membranes (third lane) because it is assumed that

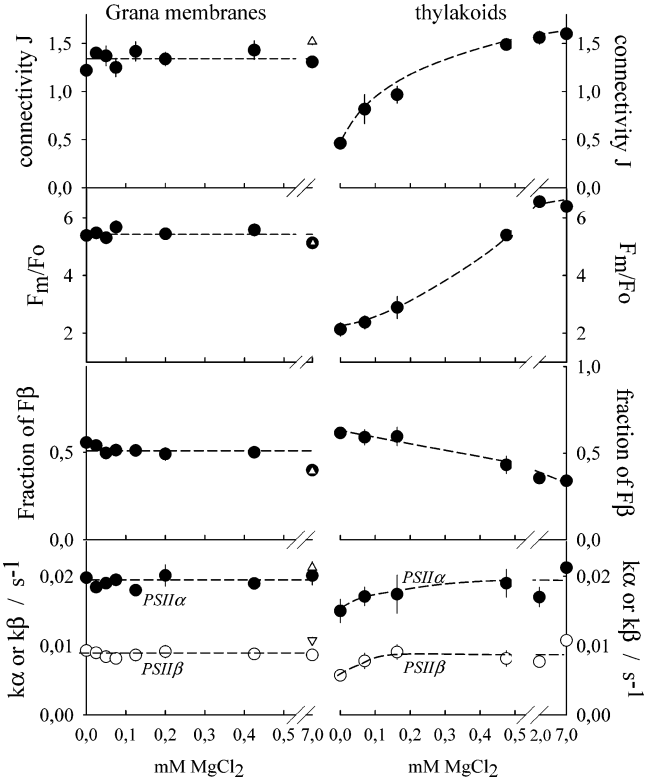

FIGURE 5: $MgCl_2$ dependency of functional PSII parameters. Data were deduced from the fitting of the chlorophyll *a* fluorescence induction curves (see Figure 4). In the left panel (grana membranes) white triangles represent untreated control membranes (not sonicated). Each point represents the mean of at least four independent determinations. Vertical bars represent the standard errors. If no error bars occur, the size of the symbol is bigger than the bar.

Table 1: Chlorophyll *a*/*b* Ratio and P700 Content of the Chloroplast and BBY Membrane Preparation[a]

	chl *a*/*b* ratio	mmol of P700/ mol of chl
BBY membranes	2.50 ± 0.10	0.96 ± 0.21
thylakoids	3.67 ± 0.10	1.96 ± 0.43

[a] The data represent the mean of four for the chlorophyll *a*/*b* ratio and two for the P700 quantification independent measurements.

core grana contain exclusively PSIIα and no PSIIβ (*14*). This can be explained by a contribution of grana margins to our BBY preparation since PSIIβ is possibly localized in this membrane domain (*15*). It is known that depending on the detergent conditions grana membrane preparations contain different amounts of margins (*29*). Here we used a relatively low detergent concentration (Triton X-100/chlorophyll = 20) to ensure highly intact grana preparation. Thus it is likely that the relative amount of margins is high. This is further indicated by the chlorophyll *a*/*b* ratio of 2.50 and the considerable amount of PSI present (Table 1). Core grana usually have a chl *a*/*b* ratio of 1.8−2.0 and in grana margins the chl *a*/*b* ratio is 3.0−3.3 (*5*). Additionally, grana margins but not core grana contain PSI (*14*). However, for the analysis of this work the significant contribution of grana margins is of minor relevance.

For intact thylakoids (Figure 5, right panel) a decrease in the $MgCl_2$ concentration is accompanied by a decline in the connectivity (*J*), the F_m/F_o ratio, and to a minor degree a

decrease in the apparent antenna size of both PSIIα and PSIIβ (k_α and k_β). The relative proportion of PSIIβ fluorescence increases slightly. These salt-induced changes in functional PSII parameters are well established for intact thylakoids (e.g., refs *22*, *44*, and *45*) and can be explained in the following way: $MgCl_2$ removal leads to destacking of grana stacks and an intermixing of the protein complexes (*20*, *21*). As a consequence the antenna systems of PSII and PSI come into excitonic contact. This results in a spillover of excitons from PSII to PSI (*46*) and a decline of the F_m/F_o ratio. Furthermore, the lateral association between LHCII and PSII is stabilized by Mg^{2+} ions because cations screen protein surface charges and enable van der Waals attraction (*47*). Thus $MgCl_2$ depletion leads to a repulsion of protein complexes and results in a decreased connectivity between PSIIα and an increase in the proportion of PSIIβ centers.

A different response to the $MgCl_2$ concentration is apparent for isolated grana thylakoids (Figure 5, left panel). None of the functional PSII parameters depends significantly on the $MgCl_2$ concentration. Especially for F_m/F_o and the proportion of PSIIβ fluorescence this is somewhat surprising since the same effects apparent for intact thylakoids are expected to be relevant for isolated grana, too. A simple explanation for these differences is given in the Discussion and is based on the limited membrane space in isolated grana compared to intact thylakoids. However, it is noteworthy that for the $MgCl_2$ concentration range under study the grana membranes change from a fully stacked to an almost completely unstacked organization (see above).

Estimation of Lateral and Transversal Exciton Energy Transfer Rates. The transfer of excitation energy between chromophores is a function of the distance between the pigments and of the angle between their transition dipole moment vectors (e.g., ref *19*). Due to the recent progress in X-ray crystallography of LHCII (*48*) and PSII cores (*49*) these data are available for the pigments bound to these proteins. However, our knowledge about the exact orientation of the proteins inside a grana stack is limited, especially concerning the relative arrangement in opposite membranes. Thus, calculations about transversal excitation energy transfer between these complexes in vivo rely on rather rough measurements of the distances between appressed membranes. Membrane to membrane distances of 3−4 nm (*50*) were calculated between adjacent lipid bilayers, whereas in ref *40* a distance of 6 nm from electron micrographs of thin sections of grana stacks was estimated. For precise calculation of the pigment−pigment distances one would have to add the distance from the edge of the membrane to the closest chlorophyll molecule. However, embedding artifacts might influence the values. A more precise estimate may be drawn from the data presented by Nield and co-workers (*10*) on isolated PSII supercomplexes examined by cryoelectron microscopy. These complexes tended to stack with their stromal surfaces, thus resembling the in vivo situation in grana stacks. By centering the actual height of LHCII (4.8 nm) as estimated by X-ray crystallography (*48*) into the density, one can calculate that the average distance between opposite LHCIIs of two stacked PSII supercores is about 2.5 nm. To get an idea of the distances between two opposite chlorophylls, one also has to consider the distance from the stromal surface of the protein to the outmost chlorophylls,

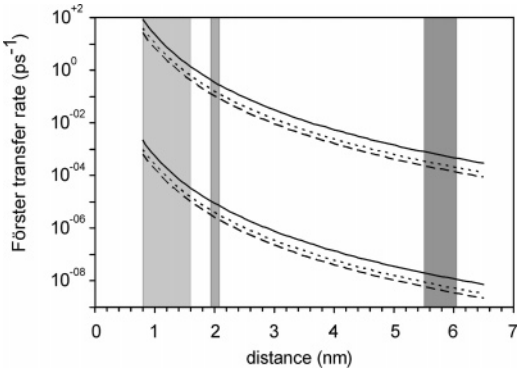

FIGURE 6: Relationship between Förster transfer rates (ps^{-1}) and chl−chl distances. The orientation factor κ was set to −2 (upper curves) and 0.01 (lower curves), respectively. Chl *a*−chl *a* transfer is shown as solid lines and chl *a*−chl *b* as dotted lines, and chl *b*−chl *b* transfer is depicted with dashed lines. The light gray bar represents chl−chl distances found in LHCII trimers; the gray bar depicts the approximate lateral and the dark gray bar the approximate transversal chl−chl distances between adjacent LHCII trimers.

which is about 1.5 nm. Thus, the minimal distance between two chlorophylls of opposite LHCII would be around 5.5 nm.

Due to the high packing density of LHCII and PSII in grana stacks the lateral distance of proteins is quite small (*30*). They even assemble into semicrystalline arrays (*26*). In those arrays, in PSII megacomplexes consisting of PSII surrounded by several LHCII trimers (*7*), and in areas consisting of only LHCII with an average distance of 8.3 nm between the centers of LHCII trimers (*51*), the distance between chlorophylls of adjacent LHCIIs is considerably smaller (around 2 nm) than found for the transversal spacing. The closest chl−chl distances are found inside LHCII, where the center-to-center distances of the neighboring chlorophylls in monomers are in the range of 0.8−1.6 nm and the smallest chl−chl distances between two monomers in a trimer are still around 1.2 nm (*48*).

Whereas the angles and thus the vectors between the pigments can be estimated for the pigments bound to LHCII, this is impossible for two pigments bound to different antenna complexes, due to our lack of knowledge concerning the precise arrangement. Thus, our comparison will consider only the range of transfer rates assuming either a rather optimal (orientation factor $\kappa = -2$) or poor orientation ($\kappa = 0.01$) of the two chlorophylls in question (see ref *19* for definitions). Figure 6 shows the distance dependence of the Förster transfer rates for the energy transfer between chl *a* and chl *a*, chl *a* and chl *b*, and chl *b* and chl *b*, respectively. The light gray bar represents the range of distances between chlorophylls inside LHCII (left) and the gray bar in the middle the distance inside PSII megacomplexes as shown by refs *7* and *26*), and the dark gray bar depicts the chl−chl distances in adjacent grana membranes. It is immediately clear that excitation energy transfer in the latter has a much lower though finite probability as the transfer rates are 2 orders of magnitude slower compared to interactions between chromophores of complexes of the same membrane or up to 4 orders of magnitude slower compared to chlorophylls inside one LHCII trimer.

DISCUSSION

Evidence That Transversal Exciton Transfer Is Missing in Grana Stacks. Recently, the first atomic force micrographs of intact thylakoid membranes (*52*) were published. In this study we apply atomic force microscopy to visualize the topography of grana membranes. The potential of this method for further structural investigations is shown in Figure 1 (right) where probably single PSII supercomplexes are discernible. It is expected that the height of a single grana membrane is determined by the height of the PSII complex, which is about 10.5 nm (*10*). In this study we determined a maximal height for destacked grana (one bilayer) of about 8 nm (mean height 6.8 nm). This reduction in height is often recognized in AFM measurements with "soft" biological probes and can be explained by a distortion of the membrane surface by the AFM tip (i.e., refs *53* and *54*) or by adhesion when measuring in air (i.e., ref *55*). Furthermore a height reduction of a membrane or of membrane stacks could be induced by the drying process. Therefore, it is likely that the absolute height values determined in this study are slightly underestimated (20−30%). However, the AFM data are self-consitent and can be used to control and quantify the degree of stacking of grana thylakoids (Figure 2). In contrast to intact thylakoid membranes, which can be destacked by incubation in buffers of low ionic strength (*21*), BBY membranes need an additional ultrasonic treatment (see Materials and Methods). Mg^{2+} ions localized between opposite grana disks are probably relatively firmly bound. Thus it is possible that energy must be supplied to release these ions and to allow for destacking (*47*). This interpretation is supported by the observation that destacking of intact thylakoids requires several hours at 4 °C but is completed in minutes at 20 °C (*40*).

An important result is that the connectivity between PSIIα (parameter *J*) in isolated grana thylakoids remains high irrespective of the degree of stacking (Figure 5, top left). The parameter *J* is a measure of the exciton transfer between neighboring PSUs (*32*). In the case of a significant contribution of transversal exciton transfer to the connectivity between PSIIα, it is expected that *J* decreases if grana are destacked. This is not observed. The data give strong evidence that transversal exciton transfer is negligible and mainly lateral energy migration is realized in grana thylakoids. Calculation of lateral and transversal Förster transfer rates based on recent structural data of PSII and LHCII supports this interpretation (Figure 6). According to this, the transversal energy transfer between adjacent chlorophylls localized in opposite grana disks is expected to be at least 100 times slower than the lateral transfer. For a rather optimal chlorophyll orientation the transversal Förster transfer time is still in the nanosecond time range (Figure 6) and thus is too slow to explain the photochemical trapping time for PSII (time from light absorption in the PSU to charge separation), which is a few hundred picoseconds (*17*). From the calculations it becomes evident that the main reason for the missing transversal exciton transfer is the large separation between chlorophylls on opposite PSUs in grana. Even under the unlikely assumption of a direct protein−protein contact of all stromal surfaces of LHCII, the transversal chl to chl distance would already be about 3 nm (see Results). In contrast, the chl to chl separation within grana disks is much smaller (Figure 6), favoring a lateral energy transfer. From the comparisons of fast photovoltage measurements on stacked and destacked thylakoids it was concluded that transversal energy transfer could occur (*25*). Considering LHCII-only patches as described in ref *26*, transversal energy transfer might take place in cases where lateral trapping becomes unlikely. This phenomenon would depend on the amount of the LHCII-only patches, which were not quantified in this study. However, our data point to a very minor significance of transversal energy migration in stacked grana membranes.

Accepting the interpretation that transversal energy transfer in grana stacks is of minor significance, the plausibility of the models postulating two distinct types of alternating membranes in a grana disk (*27*) is questionable. Without transversal exciton transfer the proposed PSII-free, only LHCII containing grana membranes transfer absorbed light energy only along the membrane plane via the grana margins to the next disk by lateral energy transfer over several hundred nanometers. This is highly unlikely. From singlet−singlet annihilation measurements on isolated LHCII aggregates it was estimated that the lateral diffusion radius for excitons is about 65 nm (*43*). Thus there would be a high probability that light energy harvested by the LHCII-only grana disks can never be used photochemically. Therefore, structural models assuming a mixed distribution of LHCII and PSII in all grana disks are more likely.

Significance of the Protein Density for the Lateral Exciton Transfer. In contrast to isolated grana membranes the connectivity parameter *J* in intact thylakoids depends strongly on the $MgCl_2$ concentration (Figure 5, top right). It is known that lateral protein interactions similar to the transversal stacking interactions are also stabilized by cations (*56*). Depletion of cations leads to a lateral separation of proteins and causes a decrease in the connectivity between PSIIα in thylakoids (*22*, *45*). At first sight it is surprising that this is not observed in isolated grana thylakoids. A simple explanation for this difference between intact thylakoids and isolated grana is that due to the high protein density in grana thylakoids a significant separation of protein complexes, necessary for a decline in the lateral connectivity, is impossible. It was estimated that about 80% of the membrane area in grana thylakoids is occupied by protein complexes (*30*). Thus it is likely that Mg^{2+} depletion leads to a loosening of protein interactions but not to a separation sufficient for a decrease in connectivity. In intact thylakoids the situation is different. By unstacking PSII and LHCII complexes can migrate from grana disks into stroma lamellae. This enables a significant separation of PSIIα and additionally intermixing with other protein complexes (PSI, ATPase), leading to a reduced connectivity. This interpretation would also explain why in isolated grana neither the apparent antenna sizes of PSIIα and PSII*β* decrease nor the fraction of PSII*β* centers increases (Figure 5).

Due to the occurrence of PSI in our grana preparation it is expected that Mg^{2+} depletion leads to an increased spillover from PSI to PSII (*46*) and similar to intact thylakoids to a decline in the F_m/F_o ratio which is not observed (Figure 5, left two rows). There are three possible explanations for the missing decline in isolated grana. First, the stoichiometry PSII/PSI is significantly reduced. From a PSII determination of our grana preparation in ref *30* and

the PSI determination in Table 1, we calculate a PSII/PSI ratio of 1.3 for intact thylakoids and of 4.1 for the BBY preparation. Thus it is expected that the spillover effect is significantly reduced in the grana preparation. Second, again the high protein density in grana stacks could prevent intermixing of protein complexes. Recently, we analyzed the lateral diffusion of PSII supercomplexes in grana disks by Monte Carlo simulations (*30*). Due to the high density of diffusion obstacles (protein complexes) the diffusion process is drastically impaired. We estimate that in 1 h the PSII supercomplex migrates only 60−70 nm. The situation is different in intact thylakoids. A complete intermixing during destacking of thylakoids (*21*) is facilitated by the presence of additional stroma areas. Third, it was reported that PSI can crystallize in isolated grana with associated margins (*57*). Possibly a protein intermixing is hindered by this aggregation.

Physiological Considerations. The results of this study do not rule out transversal exciton transfer in principle. Rather lateral energy transfer competes efficiently due to the shorter chl to chl distances. This could be ensured by both the high local intramolecular chlorophyll concentration (0.3 M; *58*) and the high protein density in grana stacks (e.g., ref *30*). It is interesting that lateral energy flow is also realized on the intramolecular level (*59*). In photosystems I (*8*) and II (*49*) as well as in LHCII (*48*), chlorophylls are arranged in two separated layers. The results in this study indicate that in the extended antenna system of photosystem II in grana stacks the intermolecular exciton transfer is mainly lateral as well. From the structural data it can be estimated that the two chlorophyll layers of PSII and LHCII have a similar position within the membrane, possibly ensuring an efficient intermolecular exciton transfer. It is to note that exciton migration in the antenna system of PSII is ultrafast and resembles a statistical diffusion process (*3*). Possibly the limitation to a two-dimensional diffusion plane is advantageous compared to a three-dimensional (lateral plus transversal) network. Thus, energy losses, e.g., by fluorescence emission, become less likely.

As discussed above, the high protein density in isolated grana disks could prevent the separation of LHCs and PSII complexes under Mg^{2+} depletion. Efficient separation is enabled in intact thylakoids possibly by additional membrane areas from stroma lamellae. This situation resembles the separation of LHCII from PSII after protein phosphorylation (*60*, *61*). Specific phosphorylation of LHCII and PSII subunits is an important regulation in the adjustment of the energy balance between PSII and PSI. Results in this study indicate that a simple loosening of protein−protein interaction in grana stacks, e.g., by protein phosphorylation, is not sufficient to decrease the excitonic pressure on the PSII antenna. Therefore, the migration of LHCII out of the stacked grana is necessary. Alternatively, intramolecular alterations in the exciton transfer efficiency of LHCII could lead to a decreased energy input to PSII (*24*).

REFERENCES

1. Jansson, S. (1994) The light-harvesting chlorophyll *a*/*b* binding proteins, *Biochim. Biophys. Acta 1184*, 1−19.
2. Green, B. R., and Durnford, D. G. (1996) The chlorophyll-carotenoid proteins of oxygenic photosynthesis, *Annu. Rev. Plant Physiol. Plant Mol. Biol. 47*, 685−714.
3. Van Grondelle, R., Dekker, J. P., Gillbro, T., and Sundstrom, V. (1994) Energy transfer and trapping in photosynthesis, *Biochim. Biophys. Acta 1187*, 1−65.
4. Jansson, S. (1999) A guide to the Lhc genes and their relatives in arabidopsis, *Trends Plant Sci. 4*, 236−240.
5. Albertsson, P.-A. (2000) The domain structure and function of the thylakoid membrane, *Recent Res. Dev. Bioenerg. 1*, 143−171.
6. Staehelin, L. A., and van der Staay, G. W. M. (1996) Structure, composition, functional organization and dynamic properties of thylakoid membranes, in *Oxygenic photosynthesis: The light reactions* (Ort, D. A., and Yocum, C. F., Eds.) pp 11−30, Kluwer, Dordrecht, The Netherlands.
7. Boekema, E. J., van Roon, H., Calkoen, F., Bassi, R., and Dekker, J. P. (1999) Multiple types of association of photosystem II and its light-harvesting antenna in partially solubilized photosystem II membranes, *Biochemistry 38*, 2233−2239.
8. Ben-Shem, A., Frolow, F., and Nelson, N. (2003) Crystal structure of plant photosystem I, *Nature 426*, 630−635.
9. Stoebel, D., Choquet, Y., Popot, J.-L., and Picot, D. (2003) An atypical haem in the cytochrome b_6f complex, *Nature 426*, 413−418.
10. Nield, J., Orlova, E. V., Morris, E. P., Gowen, B., van Heel, M., and Barber, J. (2000) 3D map of the plant photosystem II supercomplex obtained by cryoelectron microscopy and single particle analysis, *Nat. Struct. Biol. 7*, 44−47.
11. Govindjee (1995) Sixty-three years since Kautsky: Chlorophyll *a* fluorescence, *Aust. J. Plant Physiol. 22*, 131−160.
12. Bernhardt, K., and Trissl, W. (1999) Theories for kinetics and yields of fluorescence and photochemistry: how, if at all, can different models of antenna organization be distinguished experimentally?, *Biochim. Biophys. Acta 1409*, 125−142.
13. Blankenship, R. E. (2002) *Molecular Mechanisms of Photosynthesis*, Blackwell Science, Oxford.
14. Albertsson, P.-A. (2001) A quantitative model of the domain structure of the photosynthetic membrane, *Trends Plant Sci. 6*, 349−354.
15. Lavergne, J., and Briantais, J.-M. (1996) Photosystem II heterogeneity, in *Oxygenic photosynthesis: The light reactions* (Ort, D. A., and Yocum,C. F., Eds.) pp 265−287, Kluwer, Dordrecht, The Netherlands.
16. Bumba, L., and Vácha, F. (2003) Electron microscopy in structural studies of photosystem II, *Photosynth. Res. 77*, 1−19.
17. Dekker, J. P., and vanGrondelle, R. (2000) Primary charge separation in photosystem II, *Photosynth. Res. 63*, 195−208.
18. Gobets, B., and vanGrondelle, R. (2001) Energy transfer and trapping in photosystem I, *Biochim. Biophys. Acta 1507*, 80−99.
19. VanAmerongen, H., and vanGrondelle, R. (2001) Understanding the energy transfer function of LHCII, the major light-harvesting complex in green plants, *J. Phys. Chem. B 105*, 604−617.
20. Izawa, S., and Good, N. E. (1966) Effect of salts and electron transport on the conformation of isolated chloroplasts. II Electron microscopy, *Plant Physiol. 41*, 544−552.
21. Staehelin, L. A. (1976) Reversible particle movements associated with unstacking and restacking of chloroplast membranes in vitro, *J. Cell Biol. 71*, 136−158,
22. Briantais, J.-M., Vernotte, C., Olive, J., and Wollman, F.-A. (1984) Kinetics of cation-induced changes of photosystem II fluorescence and of lateral distribution of the two photosystems in the thylakoid membranes of pea chloroplasts, *Biochim. Biophys. Acta 766*, 1−8.
23. Anderson, J. M. (1999) Insights into the consequences of grana stacking of thylakoid membranes in vascular plants: a personal perspective, *Aust. J. Plant Physiol. 26*, 625−639.
24. Allen, J. F., and Forsberg, J. (2001) Molecular recognitionin thylakoid structure and function, *Trends Plant Sci. 6*, 317−326.
25. Trissl, H.-W., Breton, J., Deprez, J., and Leibl, W. (1987) Primary electrogenic reactions of photosystem II as probed by the light-gradient method, *Biochim. Biophys. Acta 893*, 305−319.
26. Boekema, E. J., van Breemen, J. F. L., van Roon, H., and Dekker, J. P. (2000) Arrangement of photosystem II supercomplexes in crystalline macrodomains within the thylakoid membrane of green plant chloroplast, *J. Mol. Biol. 301*, 1123−1133.
27. Ford, R. C., Stoylova, S. S., and Holzenburg, A. (2002) An alternative modle for photosystem II/light harvesting complex II in grana membranes based on cryo-electron microscopy studies, *Eur. J. Biochem. 269*, 326−336.

28. Berthold, D. A., Babcock, G. T., and Yocum, C. F. (1981) A highly resolved, oxygen-evolving photosystem II preparation from spinach thylakoid membranes, *Fed. Eur. Biochem. Soc. 134*, 231−234.
29. Dunahay, T. G., Staehelin, L. A., Seibert, M., Ogilvie, P. D., and Berg, S. P. (1984) Structural, biochemical and biophysical characterization of four oxygen-evolving photosystem II preparations from spinach, *Biochim. Biophys. Acta 764*, 179−193.
30. Kirchhoff, H., Tremmel, I., Haase, W., and Kubitscheck, U. (2004) Supramolecular photosystem II organization in grana thylakoid membranes: Evidence for a structured arrangement, *Biochemistry 43*, 9204−9213.
31. Lazár, D. (1999) Chlorophyll *a* fluorescence induction, *Biochim. Biophys. Acta 1412*, 1−28.
32. Lavergne, J., and Trissl, H.-W. (1995) Theory of fluorescence induction in photosystem II: Derivation of analytical expressions in a model including exction-radical-pair equilibrium and restricted energy transfer between photosynthetic units, *Biophys. J. 68*, 2474−2492.
33. Randall, P. J., and Bouma, D. (1973) Zinc deficiency, carbonic anhydrase, and photosynthesis in leaves of spinach, *Plant Physiol. 52*, 229−232.
34. Kirchhoff, H., Horstmann, S., and Weis, E. (2000) Control of the photosynthetic electron transport by PQ diffusion microdomains in thylakoids of higher plants, *Biochim. Biophys. Acta 1459*, 148−168.
35. Porra, R. J., Thompson, W. A., and Kriedermann, P. E. (1989) Determination of accurate extinction coefficient and simultaneous equations for essaying chlorophylls *a* and *b* extracted with four different solvents: verification of the concentration of chlorophyll standards by atomic absorption spectroscopy, *Biochim. Biophys. Acta 975*, 384−394.
36. Enz, C., Steinkamp, T., and Wagner, R. (1993) Ion channels in the thylakoid membrane (a patch-clamp study), *Biochim. Biophys. Acta 1143*, 67−76.
37. Kirchhoff, H., Hinz, H.-J., and Rösgen, J. (2003) Aggregation and fluorescence quenching of chlorophyll *a* of the light-harvesting complex II from spinach in vitro, *Biochim. Biophys. Acta 1606*, 105−116.
38. Klughammer, C., and Schreiber, U. (1998) Measuring P700 absorbance changes in the near infrared spectral region with a dual wavelength pulse modulation system, in *Photosynthesis: Mechanism and Effects* (Garab, G., Ed.) Vol. 5, pp 4357−4360, Kluwer, Dordrecht, The Netherlands.
39. Jones, T. A., Zou, J.-Y., Cowan, S. W., and Kjeldgaard, M. (1991) Improved methods for building protein models in electron density maps and the location of errors in these models, *Acta Crystallogr. A 47*, 110−119.
40. Arvidsson, P.-O., and Sundby, C. (1999) A model for the topology of the chloroplast thylakoid membrane, *Aust. J. Plant Physiol. 26*, 687−694.
41. Nagl, J. F., and Tristram-Nagl, S. (2000) Structure of lipid bilayers, *Biochim. Biophys. Acta 1469*, 159−195.
42. Bustamante, C., and Maestre, M. F. (1988) Statistical effects in the absorption and optical activity of particulate suspensions, *Proc. Natl. Acad. Sci. U.S.A. 85*, 8482−8486.
43. Barzda, V., Garab, G., Gulbinas, V., and Valkunas, L. (1996) Evidence for long-range excitation energy migration in macroaggregates of the chlorophyll *a*/*b* light-harvesting antenna complexes, *Biochim. Biophys. Acta 1273*, 231−236.
44. Wollman, F.-A., and Diner, B. A. (1980) Cation control of fluorescence emission, light scatter, and membrane stacking in pigment mutants of *Chlamydomonas reinhardii*, *Arch. Biochem. Biophys. 201*, 646−659.
45. Hsu, B.-D., and Lee, J.-Y. (1991) A study on the fluorescence induction curve of the DCMU-poissed chloroplast, *Biochim. Biophys. Acta 1056*, 285−292.
46. Nairn, J. A., Haehnel, W., Reisberg, P., and Sauer, K. (1982) Picosecond fluorescence kinetics in spinach chloroplasts at room temperature. Effects of Mg^{2+}, *Biochim. Biophys. Acta 682*, 420−429.
47. Barber, J. (1982) Influence of surface charges on thylakoid structure and function, *Annu. Rev. Plant Physiol. 33*, 261−295.
48. Liu, Z., Yan, H., Wang, K., Kuang, T., Zhang, J., Gui, L., An, X., and Chang, W. (2004) Crystal structure of spinach major light-harvesting complex at 2.72 Å resolution, *Nature 428*, 287−292.
49. Ferreira, K. N., Iverson, T. M., Maghlaoui, K., Barber, J., and Iwata, S. (2004) Architecture of the photosynthetic oxygen-evolving center, *Science 303*, 1831−1838.
50. Murakami, S., and Packer, S. (1970) Protonation and chloroplast membrane structure, *J. Cell Biol. 47*, 332−351.
51. Dekker, J. P., van Roon, H., and Boekema, E. J. (1999) Heptameric association of light-harvesting complex II trimers in partially solubilized photosystem II membranes, *Fed. Eur. Biochem. Soc. 449*, 211−214.
52. Kaftan, D., Brumfeld, V., Nevo, R., Scherz, A., and Reich, Z. (2002) From chloroplasts to photosynthesis: *in situ* scanning force microscopy on intact thylakoid membranes, *EMBO J. 21*, 6146−6153.
53. Pignataro, B., Chi, L. F., Gao, S., Anczykowski, B., Niemeyer, C. M., Adler, M., and Fuchs, H. (2002) Dynamic scanning force microscopy study of self-assembled DNA-protein nanostructures, *Appl. Phys. A 74*, 447−452.
54. Kühle, A., Sorensen, A. H., Zandbergen, J. B., and Bohr, J. (1998) Contrast artifacts in tapping tip atomic force microscopy, *Appl. Phys. A 66*, 329−332.
55. John, S., Noor, T. V., van der Werf, K. O., Grooth, B. G. D., Hulst, N. F. V., and Greve, J. (1997) Height anomalies in tapping mode atomic force microscopy in air caused by adhesion, *Ultramicroscopy 69*, 117−127.
56. Barber, J. (1980) Membrane surface charges and potentials in relation to photosynthesis, *Biochim. Biophys. Acta 594*, 253−308.
57. Kitmitto, A., Holzenburg, A., and Ford, R. C. (1997) Two-dimensional crystals of photosystem I in higher plant grana margins, *J. Biol. Chem. 272*, 19497−19501.
58. Kühlbrandt, W., and Wang, D. N. (1991) Three-dimensional structure of plant light-harvesting complex determined by electron crystallography, *Nature 350*, 130−134.
59. Kühlbrandt, W. (2001) Chlorophylls galore, *Nature 411*, 896−899.
60. Kruse, O. (2001) Light-induced short-term adaptation mechanisms under redox control in the PSII-LHCII supercomplexes: LHCII state transition and PSII repair cycle, *Naturwissenschaften 88*, 284−292.
61. Allen, J. F. (2003) State transitions—a question of balance, *Science 299*, 1530−1532.

BI048473W